# BENCHMARK TESTS OF JENDL-3.3 AND ENDF/B-VI DATA FILES USING MONTE CARLO SIMULATION OF THE 3 MW TRIGA MARK IIRESEARCH REACTOR

**M.Q. Huda, T.K. Chakrobortty, M.J.H. Khan and M.M. Sarker**

**Institute of Nuclear Science & Technology**
**Atomic Energy Research Establishment**
**Ganakbari, Savar, GPO Box 3787**
**Dhaka-1000, Bangladesh.**
**E-mail: quamrul@dhaka.net**

The three-dimensional continuous-energy Monte Carlo code MCNP4C was used to develop a versatile and accurate full-core model of the 3 MW TRIGA MARK II research reactor at Atomic Energy Research Establishment, Savar, Dhaka, Bangladesh. The model represents in detail all components of the core with literally no physical approximation. All fresh fuel and control elements as well as the vicinity of the core were precisely described. Validation of the newly generated continuous energy cross section data from JENDL-3.3 was performed against some well-known benchmark lattices using MCNP4C and the results were found to be in very good agreement with the experiment and other evaluations. For TRIGA analysis continuous energy cross section data from JENDL-3.3 and ENDF/B-VI in combination with the JENDL-3.2 and ENDF/B-V data files (for $^{nat}Zr$, $^{nat}Mo$, $^{nat}Cr$, $^{nat}Fe$, $^{nat}Ni$, $^{nat}Si$, and $^{nat}Mg$) at 300K evaluations were used. Full S(α,β) scattering functions from ENDF/B-V for Zr in ZrH, H in ZrH and water molecule, and for graphite were used in both cases. The validation of the model was performed against the criticality and reactivity benchmark experiments of the reactor. The MCNP calculated values for effective multiplication factor $k_{eff}$ underestimated 0.0250%Δk/k and 0.2510%Δk/k for control rods critical positions and overestimated 0.2098%Δk/k and 0.0966%Δk/k for all control rods withdrawn positions using JENDL-3.3 and ENDF/B-VI, respectively. The core multiplication factor differs appreciably (~3.3%) between the no S(α,β) (when temperature representation for free gas treatment is about 300K) and 300K S(α,β) case. However, there is ~20.0% decrease of thermal neutron flux occurs when the thermal library is removed. Effect of erbium isotope that is present in the TRIGA fuel over the criticality analysis of the reactor was also studied. In addition to the $k_{eff}$ values, the well known integral parameters: $\delta^{28}$, $\delta^{25}$, $\rho^{25}$, and $C^*$ were calculated and compared for both JENDL3.3 and ENDF/B-VI libraries using the Monte Carlo simulation of the TRIGA reactor and found very close agreement among the two libraries. Results are also reported for most of the analyses performed by JENDL-3.2 and ENDF/B-V data libraries.

## 1. Introduction

A 3 MW TRIGA MARK II research reactor was commissioned at the Atomic Energy Research Establishment, Savar, Dhaka in 1986 and it went critical on 14th September, 1986. The diffusion theory model using multigroup cross section libraries analyzed some of the reactor experimental data. [1] In most cases, it was not possible to make valid comparisons due to various geometric and analytical approximations (e.g. homogenization, multigroup cross section treatment, etc.) commonly associated with these codes. So, applications of these codes for reactor analysis require qualification from other independent codes, which to some extent are free from the above- mentioned shortcomings. Because of this need for independent assessment, the Monte Carlo technique can be beneficial. For the purpose of modeling the TRIGA MARK II reactor, the general-purpose 3-D *M*onte *C*arlo *N*-*P*article code MCNP4C [2] was chosen because of its general geometry modeling capability, correct representation of transport effects. The MCNP has the advantage of using a continuous energy cross section treatment as opposed to a multigroup approach thereby eliminating the errors in formulating few group cross sections. Continuous energy cross-section data from JENDL-3.3 and ENDF/B-VI in combination with JENDL-3.2 and ENDF/B-V data libraries (for $^{nat}Zr$, $^{nat}Mo$, $^{nat}Cr$, $^{nat}Fe$,

$^{nat}Ni$, $^{nat}Si$, and $^{nat}Mg$) at 300K evaluations were used. Full S(α,β) scattering functions from the ENDF/B-V library were used in both cases. An essential aspect of developing an accurate reactor physics model is validation. The accuracy of both the neutron transport physics as represented in MCNP and the user-defined model must be assessed. However, even though MCNP has been proven to simulate the physical interactions correctly, that does not mean that the model of TRIGA will provide accurate answers. Therefore, to build confidence, all the neutronic parameters including effective multiplication factor, in-core and ex-core neutron flux and benchmarking of reactivity experiments were performed for the fresh core to supplement and compare MCNP predicted values with the experiments. It may be mentioned that this benchmarking of Monte Carlo simulation of TRIGA reactor is one of very few low-enrichment benchmarks available.

## 2. MCNP Modeling of TRIGA

The TRIGA core consists of 100 fuel elements arranged in a concentric hexagonal array within the core shroud. The reactor is a light water cooled, graphite-reflected one, designed for continuous operation at a steady-state power level of 3000 kW (thermal). Figure 1 shows the cross sectional view of the present core arrangement of the reactor. The spaces between the rods are filled with waters that act as coolant and moderator. The repeated structure capability of MCNP was used to create a full core, three-dimensional model of TRIGA. [2] The fuel elements were modeled explicitly specifying the detailed structure of the rod to eliminate any homogenization effects. All the control rods were explicitly modeled along the active length with the exception of the drive mechanism. The central thimble was considered to be filled with water in the model and the pneumatic tube was assumed to be void. The graphite dummy elements are of the same general dimensions and construction as the fuel-moderator elements, except these elements are filled entirely with graphite. The model was extended up to ~100 cm radially containing the graphite reflector and lead shield and ~ 110 cm above and below the core centerline, which was more than sufficient to account for the neutron returning from the $H_2O$ coolant above and below the core. An annular well on the inside diameter in the top of the graphite reflector that provides for the rotary specimen rack Lazy Susan was also modeled along with the radial and tangential beam ports. Thus, it has been possible to describe the geometry of the TRIGA reactor explicitly without resorting to any approximation at all. The MCNP4C input was prepared in such a way that a very quick setup of any desired core configuration with an adequate position of all control rods is possible. A summary of the principal design parameters, material composition data and details of the modeling of the reactor can be found in Ref. 3. All geometric and material data are taken from the fabrication and shipment documentation, provided by the reactor vendor General Atomics.

## 3. Generation of Cross Section Library

Continuous energy cross-section data for all the materials present in the Monte Carlo simulation of the TRIGA reactor were generated from JENDL-3.3 using the NJOY nuclear data processing system. The Japanese Evaluated Nuclear Data Libraries (JENDL) has progressed through a number of versions; the latest version JENDL-3.3 has been tentatively released to test the validation in early 2000. [4] The cross section set at 300K was generated using NJOY99.0, [5] the latest version of NJOY, which constructs, broadens and formats the data into the appropriate form for MCNP. For heavier isotopes, resonance cross section formulae are used to calculate the elastic, capture, and fission cross sections over a defined "resonance range." Comparison of resonance integrals and thermal cross sections for $^{235}U$ and $^{238}U$ from JENDL and ENDF data libraries is shown in Table I. At higher energies in heavier nuclei, the resonances get so close together that they cannot be given separately. Instead of giving individual resonances with their energies and characteristic widths, ENDF-format evaluations give average values for the resonance spacing and the various characteristic widths, together with the probability distributions needed to describe the quantities. The self-shielded cross sections are computed by UNRESR and the probability tables are computed by PURR. The probability tables from PURR are usually processed by the ACER module and made available to the Monte Carlo code MCNP. Some modifications are required in MODER module of NJOY99.0 to process JENDL-

3.3 data of $^{238}$U nuclei comprised of covariance data. [6] Comparison of resolved and unresolved resonance energy regions for $^{235}$U and $^{238}$U isotopes from JENDL and ENDF is tabulated in Table II.

Validation of the newly generated continuous energy cross section data from JENDL-3.3 was performed against some well-known benchmark lattices using MCNP4C code and the results were found to be very good agreement with the experiment and other evaluations. Small fast reactor cores like GODIVA with hard neutron spectrum and thermal reactor core like TRX with water-moderated lattice of uranium fuel were selected. [7] Results are also reported from the analyses of these benchmark lattices based on JENDL-3.2, ENDF/B-V and ENDF/B-VI data libraries. Calculated lattice parameters are obtained from reaction rates edited for the central, asymptotic portion of the lattice. These are (with a thermal-cut energy of 0.625 eV):

$\delta^{28}$ = ratio of $^{238}$U fissions to $^{235}$U fissions.
$\delta^{25}$ = ratio of epithermal-to-thermal $^{235}$U fissions.
$\rho^{25}$ = ratio of epithermal-to-thermal $^{238}$U captures.
$C^*$ = ratio of $^{238}$U captures to $^{235}$U fissions.

These lattices directly test the $^{235}$U resonance fission integral and thermal fission cross section. They also test $^{238}$U shielded resonance capture and the thermal capture cross section. The integral parameters after leakage corrections for different lattices along with the $k_{eff}$ values are summarized in Table III. [7] The eigenvalue predictions by MCNP4C using different versions of JENDL and ENDF libraries for all three lattices are excellent. For TRX-1, the $\delta^{28}$ and $\rho^{25}$ values for JENDL-3.3 are slightly overpredicting the experimental values, but much more closely than those of ENDF/B-VI. Excellent agreement are observed for $\delta^{25}$ and $C^*$ values for both the libraries. In case of TRX-2, once again, all the integral parameters are in good agreement with the experiment. TRX-2 is a more thermal system than TRX-1 and, as a rule, evaluations agree better with the experiment, reflecting the slight overprediction of $^{238}$U resonance capture. Comparing the calculated integral parameters based on the latest version of JENDL-3.3 with the measured values and results from other evaluations for three light water benchmark lattices, it can be concluded that the performance of the newly generated continuous energy cross section library from JENDL-3.3 is quite satisfactory and offers a significant improvement compared to the other libraries. Almost all the parameters are within the experimental uncertainty limits of the measurements. So the generated continuous energy cross section data files from JENDL-3.3 library can be used for the TRIGA benchmark analysis with confidant.

## 4. Results and Discussions

The neutronic analysis of the 3 MW TRIGA MARK II benchmark experiments at AERE, Savar was performed by the three-dimensional Monte Carlo code MCNP4C using the JENDL-3.3 and ENDF/B-VI data libraries and the results are summarized in the following sections.

### A. Effective Multiplication Factor

The calculation of effective multiplication factor $k_{eff}$ was performed for the core both with and without control rods. The control rods in the former were in the critical positions and in the latter were completely withdrawn positions. The initial critical core configuration ($k_{eff}$ equal to 1.0) was obtained with critical rod height of all control rod bank positions to 37.1309% equivalent to a length of 14.146875 cm, i.e., all control rods were 23.953125 cm inserted to the active core. The estimated statistical error (1$\sigma$) was reduced below 0.03% upon 3000 cycles of iteration on a nominal source size of 3,000 particles per cycle. The comparison between the MCNP calculated $k_{eff}$ and the experimental one is shown in Table IV. The MCNP calculated values of $k_{eff}$ underestimated 0.0250%$\Delta$k/k and 0.2510%$\Delta$k/k for control rods critical positions and overestimated 0.2098%$\Delta$k/k and 0.0966%$\Delta$k/k for all control rods withdrawn positions using JENDL-3.3 and ENDF/B-VI data libraries, respectively.

B. Neutron Flux Analysis

A comparison was made between the experimentally measured peak neutron flux at the water filled central thimble (CT) and at the rotary specimen rack Lazy Susan (LS) of the reactor with the MCNP calculations and tabulated in Table V. The neutron flux, normalized to 3 MW (thermal), was calculated in MCNP that tallied the integrated neutron flux above the appropriate energy in the irradiated volume. The thermal energy range was chosen from 0 to 0.41 eV and epithermal energy range was 0.41 eV to 9.118 keV. The peak thermal neutron flux calculated by MCNP is under predicting the experimental one by ~8.46% and ~11.3% for JENDL-3.3 and ENDF/B-VI, respectively. It is also found that the MCNP predicted values for the epithermal neutron flux agree more closely with experimental values.

C. Power Distribution and Peaking Factor

The total power produced within the fuel and fuel-follower elements of the core was calculated through MCNP4C using JENDL-3.3 and ENDF/B-VI and is shown in Fig. 2. The fuel and fuel-follower element numbers are such that the fuel number 1 in the Fig. 2 represents the C1 fuel element of TRIGA core arrangement (Fig. 1) and similarly 2 & 3 represents C2 & C4 fuel elements and so on. The maximum power production of 5.6791 x $10^4$ kW and 5.5619 x $10^4$ kW are observed for JENDL-3.3 and ENDF/B-VI, respectively, within the fuel element designated by C4 (Fig. 2) and is assumed to be the hottest rod in the TRIGA core. Now the hot-rod factor is determined in MCNP using the following component values:

$$\left[\overline{P_{rod}}\Big/\overline{P_{core}}\right]_{max} = \frac{\text{Average Power Produced in the hottest Fuel Element}}{\text{Average Power in the Core}}$$

$$= 1.8930 \text{ [obtained with JENDL-3.3]}$$

$$= 1.8540 \text{ [obtained with ENDF/B-VI]}$$

This value for C4 fuel element (hot rod) is found to be in very good agreement with the calculated value of 1.8746 obtained from CITATION calculation.[1]

D. Effect of S(α,β) Library

The initial critical eigenvalue predicted by the model were 0.99975 and 0.99749 for JENDL-3.3 and ENDF/B-VI, respectively and compared well with the measured value of 1.00. For a few low-z materials, thermal scattering S(α,β) cross sections at certain temperatures are available that account for the effects of chemical binding and crystalline structure and is used in order to accurately model the neutron interactions at energies below ~ 4eV. Results of the effects of thermal library for Zr/H, H/Zr, light water and graphite are given in Table VI. The core multiplication factor differs appreciably (~3.3%) between the no S(α,β) (when temperature representation for free gas treatment is about 300K) and 300K S(α,β) case using both JENDL-3.3 and ENDF/B-VI libraries. However, there is ~20.0% decrease of thermal neutron flux occurs when the thermal library is removed, but no significant changes occur in case of epithermal neutron flux.

E. Effect of Erbium Isotope over TRIGA LEU fuel

In the U-ZrH TRIGA fuel, the temperature-hardened spectrum is used to decrease reactivity through its interaction with a low energy-resonance material. Thus, erbium, with its double resonance at ~ 0.5 eV, is used in the TRIGA LEU fuel as both a burnable poison and a material to enhance the prompt negative temperature coefficient. When the fuel-moderator material is heated, the neutron spectrum is hardened, and the neutrons have an increasing probability of being captured by the low-energy resonances in erbium. This increased parasitic absorption with temperature causes the reactivity to decrease as the fuel temperature increases. The neutron spectrum shift, pushing more of the thermal neutrons into the $^{167}$Er resonance as the fuel temperature increases, is illustrated in Fig. 3, where cold and hot neutron spectra are plotted along with the energy-dependent absorption cross section for $^{167}$Er form JENDL-3.3 and ENDF/B-VI. It may be mentioned that the isotopes of erbium have been incorporated for the first time in both JENDL-3.3 and ENDF/B-VI library. A study has also been performed regarding the effectiveness of $^{166}$Er and $^{167}$Er isotopes over the criticality calculation of TRIGA reactor using JENDL-3.3 and ENDF/B-VI and is summarized in Table VII. The MCNP calculated $k_{eff}$ value overestimated 9.48%Δk/k and 9.58%Δk/k for JENDL-3.3 and ENDF/B-VI, respectively, when erbium is absent in the TRIGA LEU fuel; whereas ~99.05% and ~96.66% of this increment is because of $^{167}$Er.

F. Study of Integral Parameters

The eigenvalue predictions by MCNP4C using different versions of JENDL and ENDF libraries for TRIGA reactor are excellent. Calculation has also been performed to study the integral parameters using the Monte Carlo Simulation of TRIGA reactor based on JENDL and ENDF data libraries and tabulated in Table VIII. All the integral parameters are found to be very close.

G. Control Rod Worth

Adequate treatment of control rods is very important in the simulation of any specific core configuration. Even small deviations of the model could eventually lead to large systematic errors of the calculated $k_{eff}$. Detailed methods and formulations used to calculate the control rod worths can be found in Ref. 3. Total control rod worths together with the experimental data are summarized in Table IX. The agreement between the MCNP predicted values and the experimentally determined values are consistent within the estimated experimental error of 10%. [3]

## 5. Conclusions

MCNP has been used to develop a versatile and accurate reactor physics model of the TRIGA MARK II research reactor. To minimize errors due to an inexact geometry model, the reactor was very thoroughly modeled. Validation of the newly generated continuous energy cross section data from JENDL-3.3 using NJOY99.0 data processing system was performed against some well-known benchmark lattices using MCNP4C code and the results were found to be in very good agreement with the experiment and other evaluations. The consistency and accuracy of the MCNP4C model of the TRIGA reactor core was established by comparing calculations to the experimental results of the benchmark experiments and found to be in good agreement.


## Acknowledgements

The authors wish to thank Dr. Makoto Takano of the Department of Fuel Cycle Safety Research, Tokai Research Establishment, JAERI, Japan for his valuable suggestions and assistance in modeling the various portions of the TRIGA reactor during his stay at AERE as a visiting scientist.


## References


1. Bhuiyan S.I. et al.: *Nucl. Tech.*, **130**, 111 (2000).
2. "MCNP – Monte Carlo N-Particle Transport Code (Version 4C)," RSICC#:CCC-700 (2000).
3. Huda M.Q. et al.: *Proc. Int. Conf. Physor2002: New Frontiers of Nucl. Tech.*, Paper No.: 9E-19, Korea, Oct. 7-10, 2002.
4. "JENDL-3.3 - The Japanese Evaluated Nuclear Data Library, version 3.3," JAERI (2000).
5. "NJOY - The Nuclear Data Processing System (Version 99.0)," RSICC#: PSR-480 (2000).
6. Nakamura N. and Kosako K. et al.: Private Communication.
7. Sitaraman S. "MCNP: Light Water Reactor Critical Benchmarks", GE Nuclear Energy, NEDO-32028 (1992).

Table I: Comparison of resonance integrals and thermal cross sections in JENDL and ENDF (barn)

| Material | Library | Resonance Integrals | | Thermal Cross sections at 2200 m/s | |
|---|---|---|---|---|---|
| | | Fission | Capture | Fission | capture |
| $^{235}U$ | JENDL3.3 | 585.1 | 98.69 | 276 | 141 |
| | ENDF/B-VI | 584.88 | 98.66 | 276.04 | 140.49 |
| | JENDL3.2 | 584.4 | 98.81 | 279 | 134 |
| $^{238}U$ | JENDL3.3 | 11.8E-06 | 2.717 | 1.72 | 277 |
| | ENDF/B-VI | 6.46E-05 | 2.72 | 1.7E-03 | 278 |
| | JENDL3.2 | 11.8E-06 | 2.717 | 1.72 | 277 |

Table II: Comparison of resolved and unresolved resonance energy regions in JENDL and ENDF (eV)

| Material | Library | Resolved Resonance Region | Unresolved Resonance Region |
|---|---|---|---|
| $^{235}U$ | JENDL3.3 | < 2250 | 2250 – 30000 |
| | ENDF/B-VI | < 2250 | < 100000 |
| | JENDL3.2 | < 500 | 500 – 30000 |
| | ENDF/B-V | < 82 | 82 – 25000 |
| $^{238}U$ | JENDL3.3 | 1.0E-05 – 10000 | 10000 – 150000 |
| | ENDF/B-VI | 1.0E-05 – 10000 | 10000 – 149000 |
| | JENDL3.2 | 1.0E-05 –10000 | 10000 – 150000 |
| | ENDF/B-V | 1.0E-05 – 4000 | 4000 – 149000 |

Table III: Summary of the MCNP4C results to the reference one for selected benchmark lattice analysis

| Lattice | Methods | $k_{eff}$ | $\delta^{28}$ | $\delta^{25}$ | $\rho^{25}$ | $C^*$ |
|---|---|---|---|---|---|---|
| GODIVA | Experiment | 1.00000 (±0.30) | - | - | - | - |
| | JENDL3.3 | 1.00329 (+0.33) | - | - | - | - |
| | ENDF/B-VI | 0.99669 (-0.33) | - | - | - | - |
| | JENDL3.2 | 1.00156 (+0.16) | - | - | - | - |
| | ENDF/B-V | 0.99814 (-0.19) | - | - | - | - |
| TRX-1 | Experiment | 1.00000 (±0.20) | 0.0946 (±0.41) | 0.0987 (±0.10) | 1.320 (±2.10) | 0.797 (±0.80) |
| | JENDL3.3 | 1.00134 (+0.13) | 0.09688 (+2.41) | 0.09835 (-0.35) | 1.352 (+2.42) | 0.790 (-0.88) |
| | ENDF/B-VI | 0.99930 (-0.07) | 0.09874 (+4.38) | 0.09943 (+0.74) | 1.382 (+4.70) | 0.796 (-0.13) |
| | JENDL3.2 | 1.00262 (+0.26) | 0.09464 (+0.04) | 0.09857 (-0.13) | 1.355 (+2.65) | 0.858 (+7.65) |
| | ENDF/B-V | 1.00071 (+0.07) | 0.09835 (+3.96) | 0.10006 (+3.96) | 1.379 (+4.47) | 0.796 (-0.13) |
| TRX-2 | Experiment | 1.00000 (±0.20) | 0.0693 (±0.35) | 0.0614 (±0.08) | 0.837 (±1.60) | 0.647 (±0.60) |
| | JENDL3.3 | 1.00095 (+0.10) | 0.06915 (-0.22) | 0.06037 (-0.22) | 0.842 (+0.60) | 0.639 (-1.24) |
| | ENDF/B-VI | 0.99887 (-0.11) | 0.06968 (+0.55) | 0.06092 (+0.55) | 0.857 (+2.39) | 0.642 (-0.77) |
| | JENDL3.2 | 1.00169 (+0.17) | 0.06726 (-2.94) | 0.06054 (-2.94) | 0.846 (+1.08) | 0.638(-1.39) |
| | ENDF/B-V | 1.00007 (+0.007) | 0.06965 (+0.51) | 0.06168 (+0.51) | 0.858 (+2.51) | 0.642 (0.77) |

Table IV: Comparison of criticality calculations to the experiment at different control rod positions

| Control Rods Positions | Method | Core Multiplication Factor $k_{eff}$ | C/E |
|---|---|---|---|
| Critical | Experiment | 1.00000 | - |
| | JENDL3.3 | 0.99975 ± 0.00027 | 0.999 |
| | ENDF/B-VI | 0.99749 ± 0.00029 | 0.997 |
| | JENDL3.2 | 1.00457 ± 0.00027 | 1.004 |
| | ENDF/B-V | 0.99599 ± 0.00027 | 0.995 |
| Withdrawn | Experiment | 1.077459 | - |
| | JENDL3.3 | 1.07972 ± 0.00028 | 1.002 |
| | ENDF/B-VI | 1.07850 ± 0.00028 | 1.000 |
| | JENDL3.2 | 1.08072 ± 0.00028 | 1.003 |
| | ENDF/B-V | 1.07646 ± 0.00029 | 0.999 |

Table V: Comparison of the MCNP4C TRIGA reactor peak neutron flux calculations to the experiment

| Method | Peak Neutron Flux (x $10^{13}$ n/cm$^2$.s) | | | | C/E | | | |
|---|---|---|---|---|---|---|---|---|
| | CT | | LS | | CT | | LS | |
| | Thermal | Epithermal | Thermal | Epithermal | Thermal | Epithermal | Thermal | Epithermal |
| Experiment | 8.3034 | 1.8842 | 0.7721 | 0.2132 | - | - | - | - |
| JENDL3.3 | 7.6007 | 1.8489 | 0.6277 | 0.2626 | 0.915 | 0.981 | 0.812 | 1.231 |
| ENDF/B-VI | 7.3631 | 1.8278 | 0.6285 | 0.2593 | 0.886 | 0.970 | 0.814 | 1.216 |
| JENDL3.2 | 7.5127 | 1.8835 | 0.6202 | 0.2607 | 0.904 | 0.999 | 0.803 | 1.222 |
| ENDF/B-V | 7.3978 | 1.7937 | 0.6287 | 0.2606 | 0.890 | 0.951 | 0.814 | 1.222 |

Table VI: Effect of thermal library (Zr/H, H/Zr, lwtr & grph) over the criticality and peak neutron flux calculation at different positions of the TRIGA reactor through MCNP4C using JENDL and ENDF

| Condition | Library | Core Multiplication Factor $k_{eff}$ | Peak Neutron Flux (x $10^{13}$ n/cm$^2$.s) | | | |
|---|---|---|---|---|---|---|
| | | | CT | | LS | |
| | | | Thermal | Epithermal | Thermal | Epithermal |
| 300K S(α,β) | JENDL3.3 | 0.99975 ± 0.00027 | 7.6007 | 1.8489 | 0.6277 | 0.2626 |
| | ENDF/B-VI | 0.99749 ± 0.00029 | 7.3631 | 1.8278 | 0.6285 | 0.2623 |
| No S(α,β) | JENDL3.3 | 1.03259 ± 0.00030 | 6.0971 | 1.7652 | 0.6325 | 0.2601 |
| | ENDF/B-VI | 1.03125 ± 0.00027 | 5.8799 | 1.8194 | 0.6218 | 0.2653 |

Table VII: Effect of Erbium Isotope over the criticality calculation of the TRIGA reactor through MCNP4C using JENDL-3.3 and ENDF/B-VI data libraries

| Condition | Library | Core Multiplication Factor $k_{eff}$ | % Δk/k |
|---|---|---|---|
| With $^{166}$Er & $^{167}$Er | JENDL3.3 | 1.07972 ± 0.00028 | - |
| | ENDF/B-VI | 1.07850 ± 0.00028 | - |
| Without $^{166}$Er & $^{167}$Er | JENDL3.3 | 1.18209 ± 0.00029 | 9.48 |
| | ENDF/B-VI | 1.18186 ± 0.00027 | 9.58 |
| Without $^{167}$Er | JENDL3.3 | 1.18109 ± 0.00030 | 9.39 |
| | ENDF/B-VI | 1.17836 ± 0.00027 | 9.26 |

Table VIII: Study of integral parameters using Monte Carlo simulation of TRIGA reactor based on JENDL and ENDF data libraries

| Library | $k_{eff}$ | $\delta^{28}$ | $\delta^{25}$ | $\rho^{25}$ | $C^*$ |
|---|---|---|---|---|---|
| JENDL3.3 | 0.99975 | 7.50564E-03 | 0.13892 | 6.53831 | 0.13415 |
| ENDF/B-VI | 0.99749 | 7.60809E-03 | 0.14099 | 6.66915 | 0.13548 |
| JENDL3.2 | 1.00457 | 7.28454E-03 | 0.13967 | 6.57643 | 0.13388 |
| ENDF/B-V | 0.99599 | 7.59845E-03 | 0.14272 | 6.55506 | 0.13366 |

Table IX: Comparison between the MCNP calculated control rod worths of TRIGA to the experiment

| Control Rod Worth ($) | Experiment (E) | JENDL3.3 | | ENDF/B-VI | |
|---|---|---|---|---|---|
| | | C | C/E | C | C/E |
| SAFETY | 2.73 ± 0.10 | 2.6324 ± 0.0541 | 0.9642 | 2.6163 ± 0.0530 | 0.9584 |
| SHIM I | 3.06 ± 0.10 | 2.8519 ± 0.0537 | 0.9320 | 2.8031 ± 0.0521 | 0.9160 |
| SHIM II | 2.82 ± 0.10 | 2.7634 ± 0.0530 | 0.9799 | 2.7455 ± 0.0536 | 0.9736 |
| SHIM III | 3.12 ± 0.10 | 2.8941 ± 0.0528 | 0.9276 | 2.8684 ± 0.0526 | 0.9194 |
| REGULATING | 2.78 ± 0.10 | 2.6821 ± 0.0539 | 0.9648 | 2.6738 ± 0.0536 | 0.9618 |
| TRANSIENT | 2.24 ± 0.10 | 2.2832 ± 0.0543 | 1.0193 | 2.3145 ± 0.0545 | 1.0333 |
| **TOTAL WORTH** | **16.75** | **16.1071** | **0.9616** | **16.0216** | **0.9565** |

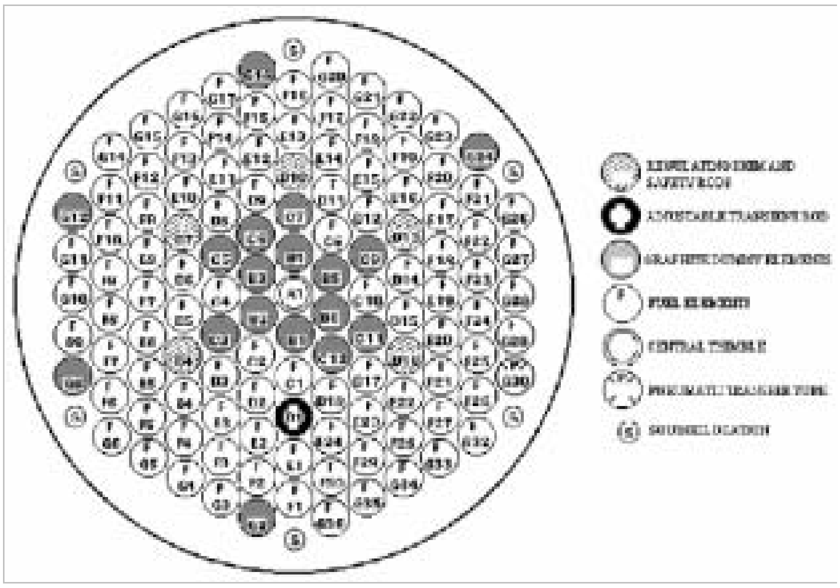

Fig. 1. Final core configuration of the 3 MW TRIGA MARK II research reactor.

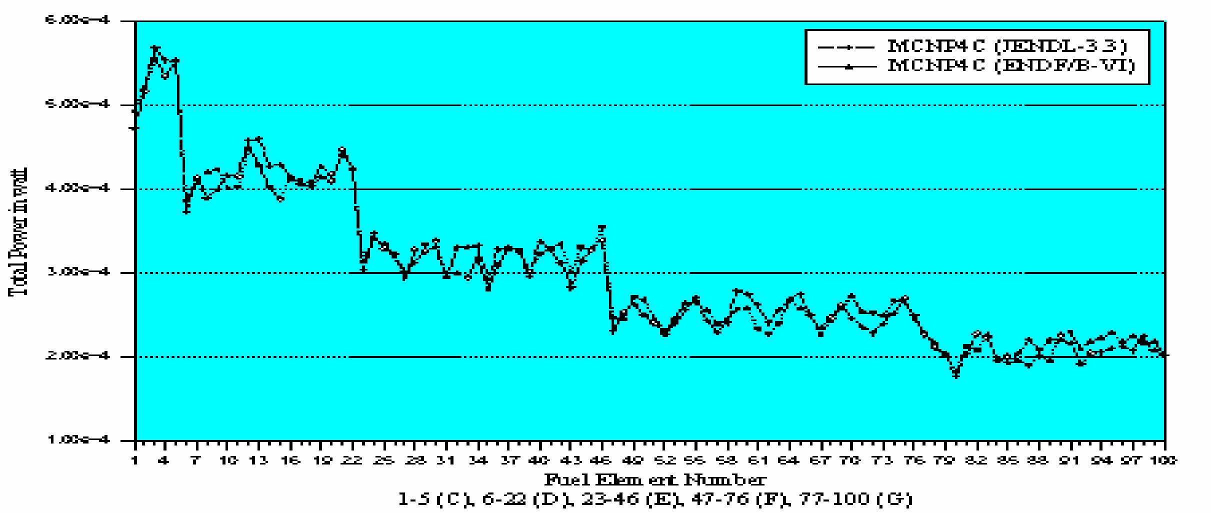


Fig. 2. Power Distribution within the Fuel and Fuel-follower Elements of TRIGA Reactor at 3 MW

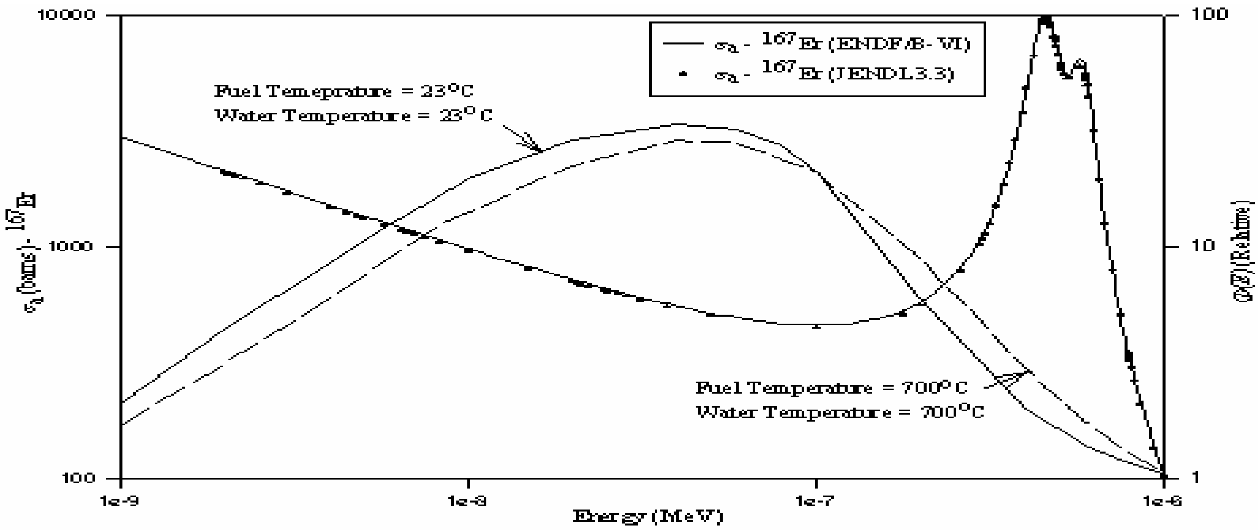


Fig. 3. Thermal neutron spectra versus fuel temperature relative to $\sigma_a$ versus energy for $^{167}$Er.